

## C-Type Starch from High-Amylose Rice Resistant Starch Granules Modified by Antisense RNA Inhibition of Starch Branching Enzyme

CUNXU WEI,<sup>†,‡</sup> BIN XU,<sup>§</sup> FENGLING QIN,<sup>‡</sup> HUAGUANG YU,<sup>§</sup> CHONG CHEN,<sup>§</sup>  
 XIANGLEN MENG,<sup>†</sup> LIJIA ZHU,<sup>†</sup> YOUPIPING WANG,<sup>‡</sup> MINGHONG GU,<sup>\*,†</sup> AND  
 QIAOQUAN LIU<sup>\*,†</sup>

<sup>†</sup>Key Laboratories of Crop Genetics and Physiology of the Jiangsu Province and Plant Functional Genomics of the Ministry of Education, <sup>‡</sup>College of Bioscience and Biotechnology, and <sup>§</sup>Testing Center, Yangzhou University, Yangzhou 225009, China

High-amylose starch is a source of resistant starch (RS) which has a great benefit on human health. A transgenic rice line (TRS) enriched amylose and RS had been developed by antisense RNA inhibition of starch branching enzymes. In this study, the native starch granules were isolated from TRS grains as well as the wild type, and their crystalline type was carefully investigated before and after acid hydrolysis. In high-amylose TRS rice, the C-type starch, which might result from the combination of both A-type and B-type starch, was observed and subsequently confirmed by multiple physical techniques, including X-ray powder diffraction, solid-state nuclear magnetic resonance, and Fourier transform infrared. Moreover, the change of starch crystalline structure from C- to B-type during acid hydrolysis was also observed in this RS-rich rice. These data could add to our understanding of not only the polymorph structure of cereal starch but also why high-amylose starch is more resistant to digestion.

**KEYWORDS:** Rice (*Oryza sativa* L.); high-amylose resistant starch granule; C-type starch; X-ray powder diffraction; solid-state nuclear magnetic resonance

### INTRODUCTION

Starch, the most important reserve component in higher plants, especially in cereal endosperm, is usually synthesized as a semi-crystalline granule containing densely packed polysaccharides with a small amount of water included. Up to now, the crystallinity of native starches has been well studied and their polymorphism has been recognized under X-ray powder diffraction (XRD) (1–3). Typically, there are three types of starch crystallinity reported, known as A-, B-, and C-type (1–3).

The A-type starch mainly exists in cereal endosperm, and their crystalline structure is mostly favored by the amylopectin with short lateral chains and closed branching points (1). The crystalline structure of B-type starch, contrary to that of A-type, is usually formed by the amylopectin with long side chains and distant branching points and can be observed in tuber crops such as potato. But there are limited reports for the C-type starch, except in smooth-seeded peas and beans (4). Usually, the C-type crystalline structure is a mixture of both A- and B-type. For example, in peas containing C-type starch, starch in the center of the granule adopts a B-type crystalline structure while the periphery is composed of the A-type crystalline structure (4).

Normally, the normal cereal starches show A-type crystalline structures as mentioned above (1), but the B-type crystalline structure is also observed, especially in high-amylose cereal starches. For example, Yano et al. (5) found that several rice mutants with high amylose content (AC, 35.4% vs 29.4% of wild type) contain starch with B-type XRD patterns. The rice line Goami 2 (previously known as Suweon 464), containing 33% of AC and about twice as much as wild type Ilpumbeyo, also presents a B-type starch structure (6). In maize, the B-type starch is also reported in the high amylose varieties (2), but not all the high-amylose cereal starches are B-type. Some rice and barley mutants with high amylose are identified to contain a typical A-type XRD pattern (7,8). Besides the typical A- and B-types, the C-type cereal starches are also presented, although in rare cases. Cheetham and Tao reported that the crystal type of maize starch could be varied from A- to B- via C-type when AC increased, and the transition occurred at about 40% (2).

Recently, we have developed several high-amylose transgenic rice lines by antisense RNA inhibition of the starch branching enzymes (SBEs) (9, 10). These transgenic rice grains are rich in resistant starch (RS) and have been proven to show a significant potential to improve the large bowel health in rats (11). Our results from microstructure and ultrastructure studies revealed that these high-amylose starch granules consist of semicomponent starch, much different from the compound starch in the starch granules from wild type rice (9).

\*To whom correspondence should be addressed. Phone, +86-514-87997217; E-mail, yzuwxcx@yahoo.com.cn (C. Wei). Phone, +86-514-87996648; E-mail, qqliu@yzu.edu.cn (Q. Liu); E-mail, gumh@yzu.edu.cn (M. Gu).

In this study, the native starch granules were further isolated from the high-amylose grains as well as their wild type, and their crystalline type was carefully investigated before and after acid hydrolysis. Interestingly, in high-amylose rice, the C-type starch structure was presented and confirmed by multiple physical techniques, including XRD,  $^{13}\text{C}$  cross-polarization magic-angle spinning nuclear magnetic resonance ( $^{13}\text{C}$  CP/MAS NMR), and attenuated total reflectance–Fourier transform infrared (ATR-FTIR). Moreover, the change of starch crystallinity from C- to B-type during acid hydrolysis was also observed in the RS-rich transgenic rice.

## MATERIALS AND METHODS

**Plant Materials.** An *indica* rice cultivar Te-qing (TQ) and its transgenic line (TRS) with high AC and RS were used in this study. TRS was generated from TQ after transgenic inhibition of two SBEs (SBEI and SBEIIb) through antisense RNA technique and held the homozygous transgene (9, 10). TRS (in T8 generation) and TQ were simultaneously cultivated in the experiment field of Yangzhou University, Yangzhou, China, in 2009, and their mature grains were used to isolate starch granules. Smooth pea (*Pisum sativum* L.) and potato (*Solanum tuberosum* L.) were obtained from a local natural food market.

**Isolation of Native Starch Granules.** Native starch granules were isolated as previously described (9) except that the samples and starch granules were not treated with NaOH. The apparent AC was determined by using a colorimetric method with iodine–potassium iodide (12).

**Preparation of Acid-Modified Starch.** The acid-modified starch was prepared according to the method of Wang et al. (13) with a slight modification. Two grams of isolated native starch were suspended in 100 mL of 2.2 M HCl solution in a sealed container. The containers were placed in an oven at 35 °C for a period from 0 to 20 days and gently shaken 3 times by hand every day in order to resuspend the sedimented granules. After the certain time of hydrolysis, the solvent was centrifuged (10 min, 3000g) and the supernatant was used for measurement of the solubilized carbohydrates to quantify the degree of hydrolysis by the anthrone– $\text{H}_2\text{SO}_4$  method (14). The undissolved residues were subsequently washed three times with  $\text{ddH}_2\text{O}$  and two times with acetone and then dried at 25 °C. The dried starches were ground into powders and passed through a 100-mesh sieve for further use. The recovery yield (wt %) of the starch after acid hydrolysis was calculated based on the change of dried starch after and before hydrolysis.

**Hydrolysis of Native Starch Granules by  $\alpha$ -Amylase.** The  $\alpha$ -amylase degraded starch granules were prepared according to the method described by Li et al. (15) with a slight modification. Isolated native starches (50 mg) were suspended in 5 mL of 0.1 M phosphate sodium buffer (pH 6.9) containing 0.006 M NaCl. *Bacillus licheniformis*  $\alpha$ -amylase (Sigma-Aldrich) was added, with a final concentration of 0.01% (w/v). The amylolysis was carried out in an oven at 37 °C for a period. After the desired time of hydrolysis, undissolved residues were isolated by centrifugation (10 min, 3000g), and the supernatant was measured for solubilized carbohydrates. The residues were dried and the recovery yield after enzyme hydrolysis calculated as above.

**XRD Analysis.** XRD analysis of isolated native and acid modified starch granules was carried out on an XRD (D8, Bruker, Germany) according to the published method (16). The samples were exposed to the X-ray beam at 200 mA and 40 kV. The scanning region of the diffraction angle ( $2\theta$ ) was from 3° to 40° with a step size of 0.02° and a count time of 0.8 s. All the specimens were stored in a desiccator, where a saturated solution of NaCl maintained a constant humidity atmosphere (relative humidity (RH) = 75%) for 1 week at 25 °C before measurements.

**ATR-FTIR Measurement.** ATR-FTIR measurement was carried out according to the method (17) with a slight modification. The spectra were obtained using a Varian 7000 FTIR spectrometer with a DTGS detector equipped with a ATR single reflectance cell containing a germanium crystal (45° incidence-angle) (PIKE Technologies, USA). For each measurement, 64 scans with a 4  $\text{cm}^{-1}$  resolution were coadded before Fourier transformation. The spectrum of water recorded in the same condition was subtracted from the sample spectra. Spectra were corrected by a baseline in the region from 1200 to 800  $\text{cm}^{-1}$  before deconvolution was applied using Resolutions Pro. The assumed line shape was Lorentzian with a half-width

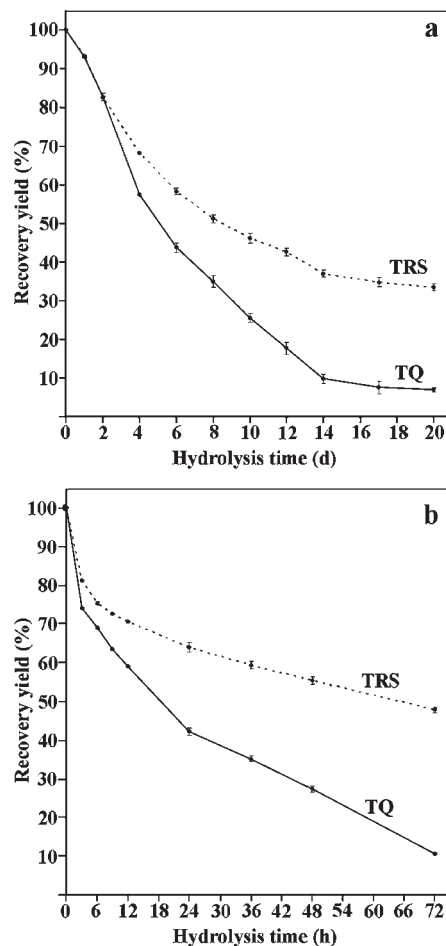


**Figure 1.** Recovery yield of starches after acid hydrolysis (a) and  $\alpha$ -amylase hydrolysis (b).

of 26  $\text{cm}^{-1}$  and a resolution enhancement factor of 2.0. IR absorbance values at 1047, 1022, and 995  $\text{cm}^{-1}$  were extracted from the spectra after water subtraction, baseline correction, and deconvolution.

**Solid-State  $^{13}\text{C}$  CP/MAS NMR Analysis.** High-resolution solid-state  $^{13}\text{C}$  CP/MAS NMR experiments were carried out at  $B_0 = 9.4$  T on a Bruker AVANCE III 400 WB spectrometer. The corresponding  $^{13}\text{C}$  resonance frequencies were 100.6 MHz. Samples were packed in a 7 mm  $\text{ZrO}_2$  rotor and spun at the magic angle (54.7°) with 6 kHz of spin rate.  $^1\text{H}$ – $^{13}\text{C}$  CP/MAS spectra were recorded with a contact time of 1.2 ms and a recycle delay of 2 s. The chemical shifts were referenced to tetramethylsilane (TMS) at 0 ppm. Typically, 8000–12000 transients were accumulated for the  $^{13}\text{C}$  spectra. All the specimens were stored in a desiccator, where a saturated solution of NaCl maintained a constant humidity atmosphere (RH = 75%) atmosphere for 1 week at 25 °C before measurements.

## RESULTS

**High AC in Isolated TRS Native Starch.** To avoid the effect of enzyme or alkaline treatment on starch crystalline structure during starch isolation, we isolated the native starch from mature rice grains without enzyme and alkaline treatment in which the samples and starch granules were only treated with water. The isolated native starches were identified to have no damage on granules (data not shown). In TRS rice, the  $\lambda_{\text{max}}$  (maximum absorption wavelength) and blue value of iodine–starch complex were significantly higher than those of wild type TQ, and as expected, the AC of TRS native starch was nearly twice (58.32% vs 29.98%) as much as that of the isolated native starch from wild type rice grains.

**High Resistance to Acid and Enzyme Hydrolysis of TRS Native Starch.** Figure 1 shows the recovery yield of native starch after

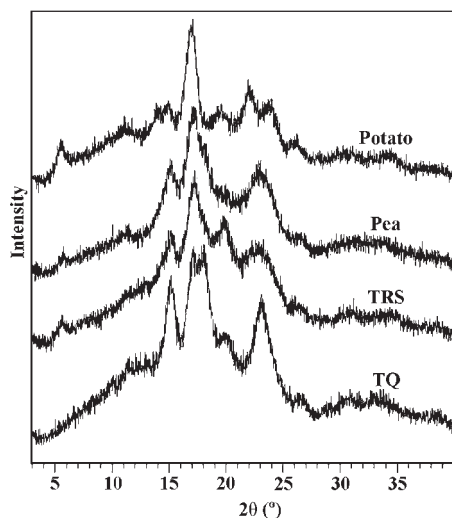


Figure 2. XRD spectra of native starches.

different times of acid or enzyme hydrolysis. For either TRS or TQ native starch, the residual starch was gradually decreased with the passage of hydrolysis time, but after 20 days of acid hydrolysis, the recovery yield of TRS starch (33.5%) was significantly higher than that (6.9%) of normal TQ starch (Figure 1a). The high recovery of residual starch in TRS rice was also observed after  $\alpha$ -amylase hydrolysis (Figure 1b). During the time course of hydrolysis, TQ starch was more readily hydrolyzed than TRS starch. After 72 h, only about 52% of the TRS native starch was hydrolyzed, whereas nearly 89% of the TQ normal starch was digested. These results suggested that TRS starch had a much higher resistance to either acid or enzyme hydrolysis than TQ starch.

**The XRD Pattern of TRS Native Starch Similar to That of Pea C-Type Starch.** The XRD patterns of native starches of TQ, TRS, pea, and potato are presented in Figure 2. These XRD patterns were carefully compared with known diffraction patterns of A-, B-, and C-type crystallinity (1, 2). The normal native starch from TQ rice grain showed strong reflection at  $2\theta$  about  $15^\circ$  and  $23^\circ$  and an unresolved doublet at  $17^\circ$ ,  $18^\circ$   $2\theta$ , which was very close to the typical A-type XRD pattern in most ordinary cereal starches (1, 2). The potato starch presented the strongest diffraction peak at around  $17^\circ$   $2\theta$  and a few small peaks at around  $2\theta$  values of  $24^\circ$ ,  $22^\circ$ , and  $15^\circ$ . An additional peak also appeared at about  $5^\circ$   $2\theta$ . These spectra were typical characteristics of B-type starch from tuber crops (1, 2). The pea starch had been reported to be a typical C-type crystallinity revealed by XRD (1, 2). On the pea starch XRD spectra, only one peak appeared at  $23^\circ$   $2\theta$ , which was indicative of the A-type pattern, while the peak at around  $5^\circ$   $2\theta$  was the characteristic of B-type pattern (1, 2). When compared with the above three type crystallinity, the XRD pattern of TRS native starch was basically the same as that of pea starch. TRS starch generally showed the presence of a B-type pattern. However, the presence of some additional A-type peaks indicated that it was a mixture of A- and B-type patterns. Thus TRS starch was classed as a C-type crystallinity. It was noteworthy that the scattering intensities for  $15^\circ$  and  $23^\circ$   $2\theta$  diffraction peaks decreased, whereas a sharp reflection peak at angles of  $20^\circ$   $2\theta$  was observed in TRS starch. The peak of  $20^\circ$   $2\theta$  was a typical amylose–lipid complex diffraction peak (1, 2), which was in agreement with the result of high AC in TRS starch.

**ATR-FTIR Spectra of TRS Native Starch.** The development of sampling devices like ATR-FTIR combined with procedures for spectrum deconvolution provided opportunities for the study of

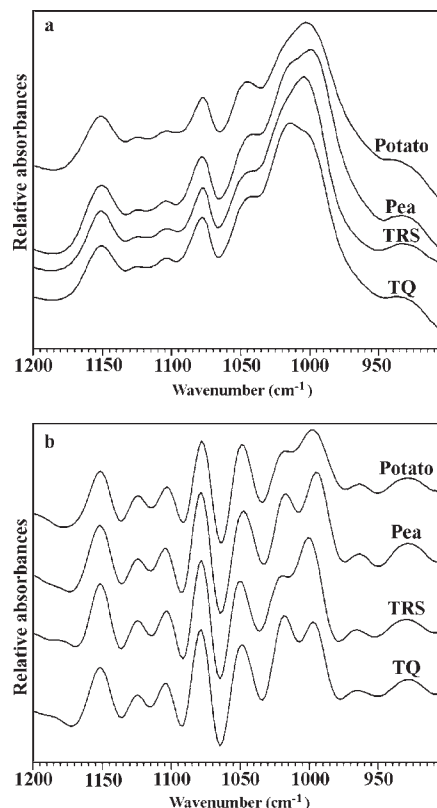


Figure 3. Original (a) and deconvoluted (b) ATR-FTIR spectra of native starches.

Table 1. IR Ratio of the Absorbances 1045/1022 and 1022/995  $\text{cm}^{-1}$  for Native Starches

	IR ratio 1045/1022 ( $\text{cm}^{-1}$ )	IR ratio 1022/995 ( $\text{cm}^{-1}$ )
TQ	0.69	1.67
TRS	0.89	0.60
pea	0.80	0.78
potato	1.09	0.75

starch external region structure (17). The original and deconvoluted ATR-FTIR spectra in the region  $1200\text{--}900\text{ cm}^{-1}$  of four native starch samples are given in Figure 3. The bands at  $1045$  and  $1022\text{ cm}^{-1}$  had been linked with order/crystalline and amorphous regions in starch, respectively (17). The ratio of absorbance  $1045/1022\text{ cm}^{-1}$  was used to quantify the degree of order in starch samples. Intensity ratios of  $1045/1022$  and  $1022/995\text{ cm}^{-1}$  might therefore be useful as a convenient index of FTIR data in comparisons with other measures of starch conformation (18). The relative intensities of FTIR bands at  $1045$ ,  $1022$ , and  $995\text{ cm}^{-1}$  were recorded from the baseline to peak height, and the ratios for  $1045/1022$  and  $1022/995$  were calculated as shown in Table 1.

On the basis of both the spectra and calculated data, the ATR-FTIR characteristics of TRS starch was much close to those of pea or potato starch, especially on the IR ratio of  $1045/1022$  or  $1022/995\text{ cm}^{-1}$ . In TRS starch spectra, the band at  $1022\text{ cm}^{-1}$  was less pronounced than in TQ and pea, which was similar to that in potato (Figure 3). These results also implied that TRS starch was a C-type starch, a mixture of A-type and B-type starches, which was in qualitative agreement with the data from XRD analysis.

**Solid-State NMR Spectra of Native Starch.** The solid-state  $^{13}\text{C}$  CP/MAS NMR patterns for native TQ and TRS starches are presented in Figure 4. Substantial similarities were observed in the spectra with high resolved resonances. The resonances at  $61.8\text{ ppm}$  was assigned to C-6, and the large signal around  $68\text{--}78\text{ ppm}$  was

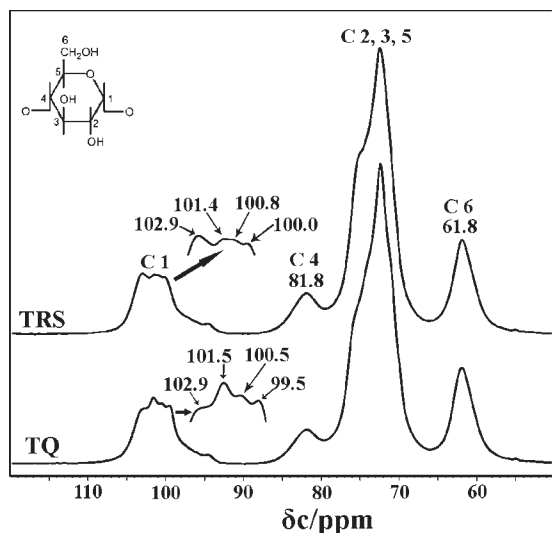


Figure 4.  $^{13}\text{C}$  CP/MAS NMR spectra of native starches.

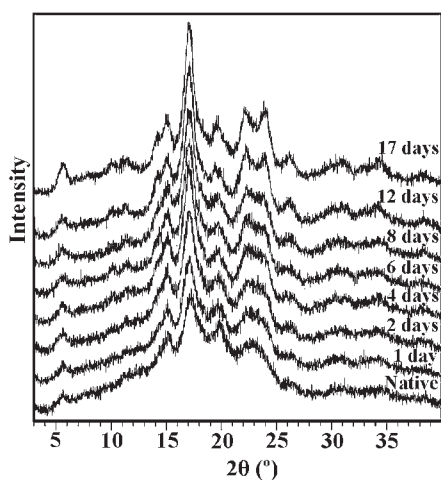


Figure 5. XRD spectra of TRS starches before and after various acid hydrolysis times.

collectively associated with C2, C3, and C5 sites. The resonance at 81.8 ppm was associated with C4 site, and the resonance at around 100–103 ppm was associated with C1 site. Except the above peaks, the weak peak appeared at 94.3 ppm could arise from the amorphous areas for C1. These assignments of the resonances were based on the literature reports (19, 20).

Two remarkable differences were observed between the  $^{13}\text{C}$  CP/MAS NMR patterns for native TQ and TRS starches. First, the C1 resonances of TQ starch occurred as triplets, which was a typical A-type characteristic (19, 20). The C1 resonances of TRS starch also occurred as inconspicuous triplets, especially weak peak at 101.4 ppm, which showed that TRS starch was a C-type crystal with dominant A-type crystalline structure. The second difference was the intensity of the resonance at 102.9 ppm. The peak at 102.9 ppm appeared only as a shoulder on the downfield C-1 resonance in TQ starch, however, that in TRS appeared as a strong peak, which showed that the content of amylose–lipid complex was higher in TRS than that in TQ.

#### Change of Crystal Type of TRS Starch during Acid Hydrolysis.

The XRD patterns of acid-modified TRS starches and their native counterpart are shown in Figure 5. One striking difference was observed for the peak at around  $2\theta$  value of  $23^\circ$  among the XRD spectra of TRS starch after different time of acid hydrolysis.

Native C-type starch from TRS grain showed only one broad peak at  $23^\circ 2\theta$ . The peak became broad from 2 to 6 days of hydrolysis and then split into two peaks at  $22^\circ$  and  $24^\circ$ , which were the typical B-type characteristics (1, 2). The disappearance of the characteristic A-type diffraction peak and the development of typical B-type diffraction peak showed that the crystal type of native TRS starch might change from typical C-type to B-type during acid hydrolysis.

#### DISCUSSION

The crystallinity of native starch can be classified to A-, B-, and C- types (1, 2). The C-type starch is usually a combination of A- and B-types, especially in maize, with about 40% of amylose (2). Up to now, in most of the reported high-amylose rice mutants, endosperm starches are characterized as a B-type pattern revealed by XRD analysis (5, 6). In this study, the starch from our developed high-amylose rice TRS was demonstrated as the C-type not only by XRD analysis but also confirmed by the  $^{13}\text{C}$  CP/MAS NMR and ATR-FTIR techniques.

$^{13}\text{C}$  solid-state NMR has been employed in examining the structure of different type starches. In the spectra, most of the resonances cannot be distinguished or have not been assigned among the A-, B-, and C-type starches, but the C-1 carbon atoms have chemical shifts characteristic for each type starch. For the A-type starch, which has three nonidentical sugar residues, the C-1 peak region is a cluster of three peaks at  $\sim 102$ , 101, and 100 ppm, respectively. For the B-type starch, which has two nonidentical sugar residues, the C-1 peak signal is a cluster of two peaks at  $\sim 101$  and 100 ppm, respectively. Because C-type starch has the characteristics of both A- and B-type crystalline structure, C-1 spectra of the C-type starch always shows a mixed pattern of both A- and B-types. The resonances in the spectra of C-type starch mainly depend on the relative proportions of A- or B-type crystallinity in the sample (20). In general, the C-type starch shows triplets C-1 spectra if the A-type crystalline structure is predominant in the sample, and two-peak C-1 spectra if the B-type crystalline structure is predominant (19, 20). In present study, the TRS starch showed inconspicuous triplets C-1 spectra (Figure 5), which implied that TRS starch existed a C-type crystallinity with dominant A-type crystalline structure.

The crystalline property of starch can be changed by acid treatment, which is very helpful to understand the fine structure of starch granules (13). In the present study, during or after acid treatment of TRS native starch, the XRD characteristic at A-type diffraction peak disappeared while the typical B-type diffraction peak came out. These phenomena indicate that the crystal type of TRS starch changed from typical C-type to B-type after acid modification. Our result was quite different from other reports (13, 16, 21). For example, the acid-modified corn starches exhibit the same crystalline type as that of its native starch (21), while the crystal type of pea and Chinese yam starches changes from C-type to A-type after acid hydrolysis (13, 16). This structure change of our TRS starch during acid treatment might be due to the degradation of A-type crystalline starch first or faster than that of B-type starch.

Resistant starch refers to the portion of starch and/or starch products that are difficult to digest when they pass through the gastrointestinal tract (22). The proportion of RS will be increased when the diet starch carries more granular structure naturally resistant to digestion (23). In our TRS grains, there is not only high level of amylose but also of RS (9, 10). As expected, the TRS starch showed a higher resistance to either acid or enzyme hydrolysis than that of its wild type starch (Figure 1). This might

be attributed to not only the high amylose but also the special granular structure of TRS starch. Our previous experiments showed that the starch granules from the regular rice TQ were organized as compound starches and dissociated to separate individual starches during starch isolation, while starch granules from TRS were organized as semicompound starches with a thick continuous band encircling the entire circumference of the granules (9). The sizes of TRS semicompound starches are larger than that of TQ individual starches, so TRS starches had a lower rate of acid hydrolysis than TQ starches, presumably due to their smaller surface area per unit weight. Also, high amylose starch was reported to be less susceptible to acid hydrolysis than normal and waxy starches. It was suggested that the highly compact amorphous regions in high amylose starch granules, resulting from extensive interchain associations of amylose polymers, prevented penetration of acid into the granules (24). TRS starch had high concentration of amylose in both the hilum and encircling band (9), which might partly explain why it was highly resistant to acid hydrolysis.

It is reported that the amount of native starch hydrolysis by amylase is inversely related to the amylose content (15). Moreover, the double helices in starch granules always prefer to form a crystalline structure that resists to enzyme hydrolysis (25–27). Both crystalline regions and double helices themselves can increase the resistance to amylase hydrolysis. This probably explains, at least in part, why high amylose starch resists amylase digestion more than native or waxy starches even though they were less crystalline (25–27). Otherwise, the A-, B- and C-types of starches show different susceptibilities to  $\alpha$ -amylase hydrolysis. Generally, the B- or C-type starch shows more resistance to enzyme hydrolysis than that of A-type (25, 28). This might be why the TRS C-type starch in the present study had a high resistant ability to  $\alpha$ -amylase digestion.

In conclusion, the high-amylose TRS starch was investigated by using XRD,  $^{13}\text{C}$  CP/MAS NMR, and ATR-FTIR techniques and subsequently confirmed to be C-type crystalline structure, which resulted from the combination of both A-type and B-type starch. During acid hydrolysis, the crystal type of TRS starch could be changed from C- to B-type. These data could add to our understanding of not only the polymorph structure of rice starch, especially of high amylose starch, but also why high amylose starch more resistant to digestion.

#### ABBREVIATIONS USED

AC, amylose content; ATR-FTIR, attenuated total reflectance-Fourier transform infrared;  $^{13}\text{C}$  CP/MAS NMR,  $^{13}\text{C}$  cross-polarization magic-angle spinning nuclear magnetic resonance; RS, resistant starch; SBE, starch branching enzyme; TQ, Te-qing (wild type rice cultivar); TRS, transgenic RS rice line; XRD, X-ray powder diffraction.

#### ACKNOWLEDGMENT

We are very grateful to Prof. Yong-Cheng Shi from Kansas State University for helpful discussions, and to the reviewers for valuable comments and corrections.

#### LITERATURE CITED

- Buléon, A.; Colonna, P.; Planchot, V.; Ball, S. Starch granules: structure and biosynthesis. *Int. J. Biol. Macromol.* **1998**, *23*, 85–112.
- Cheetham, N. W. H.; Tao, L. Variation in crystalline type with amylose content in maize starch granules: an X-ray powder diffraction study. *Carbohydr. Polym.* **1998**, *36*, 277–284.
- Imberty, A.; Buleon, A.; Vinh, T.; Perez, S. Recent advances in knowledge of starch structure. *Starch/Stärke* **1991**, *43*, 375–384.
- Bogracheva, T. Y.; Morris, V. J.; Ring, S. G.; Hedley, C. L. The granular structure of C-type pea starch and its role in gelatinization. *Biopolymers* **1998**, *45*, 323–332.
- Yano, M.; Okuno, K.; Kawakami, J.; Satoh, H.; Omura, T. High amylose mutants of rice, *Oryza sativa* L. *Theor. Appl. Genet.* **1985**, *69*, 253–257.
- Kang, H. J.; Hwang, I. K.; Kim, K. S.; Choi, H. C. Comparative structure and physicochemical properties of Ilpumbyeo, a high-quality japonica rice, and its mutant, Suweon 464. *J. Agric. Food Chem.* **2003**, *51*, 6598–6603.
- Yang, C. Z.; Shu, X. L.; Zhang, L. L.; Wang, X. Y.; Zhao, H. J.; Ma, C. X.; Wu, D. X. Starch properties of mutant rice high in resistant starch. *J. Agric. Food Chem.* **2006**, *54*, 523–528.
- Song, Y.; Jane, J. Characterization of barley starches of waxy, normal, and high amylose varieties. *Carbohydr. Polym.* **2000**, *41*, 365–377.
- Wei, C. X.; Qin, F. L.; Zhu, L. J.; Zhou, W. D.; Chen, Y. F.; Wang, Y. P.; Gu, M. H.; Liu, Q. Q. Microstructure and ultrastructure of high-amylose rice resistant starch granules modified by antisense RNA inhibition of starch branching enzyme. *J. Agric. Food Chem.* **2010**, *58*, 1224–1232.
- Zhu, L. J. Studies on starch structure and functional properties of high-amylose transgenic rice and different waxy rice varieties. Ph.D. dissertation. Yangzhou University, Yangzhou, China, 2009.
- Li, M.; Piao, J. h.; Liu, Q. Q.; Yang, X. G. Effects of the genetically modified rice enriched with resistant starch on large bowel health in rats. *Acta Nutr. Sin.* **2008**, *30*, 588–591.
- Juliano, B. O. A simplified assay for milled-rice amylose. *Cereal Sci. Today* **1971**, *16*, 334–340.
- Wang, S. J.; Yu, J. L.; Yu, J. G. The semi-crystalline growth rings of C-type pea starch granule revealed by SEM and HR-TEM during acid hydrolysis. *Carbohydr. Polym.* **2008**, *74*, 731–739.
- Viles, F. J.; Silverman, L. Determination of starch and cellulose with anthrone. *Anal. Chem.* **1949**, *21*, 950–953.
- Li, J. H.; Vasanthan, T.; Hoover, R.; Rosnagel, B. G. Starch from hull-less barley: V. In-vitro susceptibility of waxy, normal, and high-amylose starches towards hydrolysis by  $\alpha$ -amylases and amyloglucosidase. *Food Chem.* **2004**, *84*, 621–632.
- Wang, S. J.; Yu, J. L.; Zhu, Q. H.; Yu, J. G.; Jin, F. M. Granular structure and allomorph position in C-type Chinese yam starch granule revealed by SEM,  $^{13}\text{C}$  CP/MAS NMR and XRD. *Food Hydrocolloids* **2009**, *23*, 426–433.
- Sevenou, O.; Hill, S. E.; Farhat, I. A.; Mitchell, J. R. Organisation of the external region of the starch granule as determined by infrared spectroscopy. *Int. J. Biol. Macromol.* **2002**, *31*, 79–85.
- Htoon, A.; Shrestha, A. K.; Flanagan, B. M.; Lopez-Rubio, A.; Bird, A. R.; Gilbert, E. P.; Gidley, M. J. Effects of processing high amylose maize starches under controlled conditions on structural organization and amylase digestibility. *Carbohydr. Polym.* **2009**, *75*, 236–245.
- Cheetham, N. W. H.; Tao, L. Solid state NMR studies on the structural and conformational properties of natural maize starches. *Carbohydr. Polym.* **1998**, *36*, 285–292.
- Bogracheva, T. Y.; Wang, Y. L.; Hedley, C. L. The effect of water content on the ordered/disordered structures in starches. *Biopolymers* **2001**, *58*, 247–259.
- Wang, Y. J.; Truong, V. D.; Wang, L. F. Structures and rheological properties of corn starch as affected by acid hydrolysis. *Carbohydr. Polym.* **2003**, *52*, 327–333.
- Nugent, A. P. Health properties of resistant starch. *Nutr. Bull.* **2005**, *30*, 27–54.
- Rahman, S.; Bird, A.; Regina, A.; Li, Z.; Ral, J. P.; McMaugh, S.; Topping, D.; Morell, M. Resistant starch in cereals: exploiting genetic engineering and genetic variation. *J. Cereal Sci.* **2007**, *46*, 251–260.
- Li, J. H.; Vasanthan, T.; Rosnagel, B.; Hoover, R. Starch from hull-less barley: II. Thermal, rheological and acid hydrolysis characteristics. *Food Chem.* **2001**, *74*, 407–415.

- (25) Gérard, C.; Colonna, P.; Buléon, A.; Planchot, V. Amylolysis of maize mutant starches. *J. Sci. Food Agric.* **2001**, *81*, 1281–1287.
- (26) Tester, R. F.; Karkalas, J.; Qi, X. Starch structure and digestibility enzyme–substrate relationship. *World Poultry Sci. J.* **2004**, *60*, 186–195.
- (27) Cooke, D.; Gidley, M. J. Loss of crystalline and molecular order during starch gelatinization—origin of the enthalpic transition. *Carbohydr. Res.* **1992**, *227*, 103–112.
- (28) You, S.; Izydorczyk, M. S. Comparison of the physicochemical properties of barley starches after partial  $\alpha$ -amylolysis

and acid/alcohol hydrolysis. *Carbohydr. Polym.* **2007**, *69*, 489–502.

---

**Received for review January 29, 2010. Revised manuscript received March 22, 2010. Accepted May 17, 2010. This study was financially supported by grants from the National Natural Science Foundation of China (30828021, 30300215), the Ministry of Science and Technology (2006AA10A102, 2009ZX08011-003B), the Government of Jiangsu Province (BK2009186, 06KJA21018), and the China Postdoctoral Science Foundation (20090451252).**